Surface and guided wave polariton modes of magnetoplasma effective films in the Voigt geometry

1995 J. Phys.: Condens. Matter 7 7023

(http://iopscience.iop.org/0953-8984/7/35/009)

J. Phys.: Condens. Matter 7 (1995) 7023–7035. Printed in the UK

Surface and guided wave polariton modes of magnetoplasma effective films in the Voigt geometry

F G Elmzughi

Department of Physics, University of Essex, Colchester CO4 3SQ, UK
Department of Physics, Al-Fatah University, Post Box 13450, Tripoli, Libya

Received 1 May 1995, in final form 6 June 1995

Abstract. A theoretical discussion of the retarded electromagnetic modes of an effective magnetoplasma film is described. The effective film is characterized by an effective dielectric tensor, and we deal with the Voigt configuration (propagation transverse to the applied magnetic field) for both a symmetric and an asymmetric film. The numerical results show that for a symmetric effective film, dispersion curves for both surface modes and guided waves are reciprocal, $\omega(+k) = \omega(-k)$, but the field profiles are different for $+k$ and $-k$. The dispersion curves for the asymmetric effective film are non-reciprocal, and the field profiles are different. Numerical illustrations are given for a GaAs/AlAs superlattice.

1. Introduction

In recent years there has been considerable interest in the excitations of superlattice structures consisting of thin alternating layers of material. In particular it was realized by Raj and Tilley (1985) that, for the description of the electromagnetic modes of these structures (polaritons), the free space wavelength λ is much greater than the superlattice period D.

The same results were obtained by Agranovich and Kravtsov (1985), using the standard boundary conditions that require the continuity of the tangential components of the electric field E and the normal components of the displacement vector D. The far-infrared properties of doped semiconductor superlattices in the presence of a magnetic field B_0 (Oliveros *et al* 1993, Elmzughi *et al* 1995) show a number of features additional to those found in the absence of a field (Dumelow *et al* 1993). The propagation of surface waves is non-reciprocal (Camley 1987), which means that the frequency changes when the direction of travel is reversed. Non-reciprocity is a consequence of the non-zero off-diagonal elements in the effective dielectric tensor proportional to B_0.

In this paper we discuss the surface and guided wave polariton modes that propagate in a magnetoplasma *effective* thin film. A substantial account of magnetoplasma thin films has already been given by Kushwaha and Halevi (1987a,b, 1988). In these papers the authors dealt with the Faraday geometry (B_0 in the plane of the film along the propagation), the Voigt geometry (B_0 in the plane and perpendicular to the direction of propagation), and the perpendicular geometry (B_0 normal to the surface of the film). Further work dealt with the interaction between the magnetoplasma polaritons and the optic phonons in the substrate (Kushwaha and Halevi 1987c). A full discussion of surface and guided wave modes for one- and two-component magnetoplasmas has already been given by Elmzughi and Tilley (1994) in the Voigt geometry.

0953-8984/95/357023+13$19.50

In this paper we give, for the first time, a general theory of electromagnetic modes in an anisotropic magnetoplasma dielectric *effective* film, for both surface and guided wave modes in the Voigt geometry. It should be pointed out that in the absence of an applied magnetic field the behaviour of the effective medium is uniaxial, with the normal to the layers as the uniaxis (Dumelow and Tilley 1993, Dumelow *et al* 1993).

The remainder of the paper is organized as follows. In section 2 the bulk dispersion equation is derived since it defines the regions in the frequency–wavevector plane in which surface and guided waves can exist. Therefore we present a brief derivation of the bulk dispersion relation. Surface polariton modes propagate on the interface between the magnetoplasma and vacuum, in the frequency intervals that form stop bands for the bulk modes. In an effective film, surface-like modes propagate in the same windows defined by the intervals of the stop bands for the bulk modes. For this reason section 2 also contains a discussion of the surface modes of a semi-infinite effective medium superlattice. The dispersion equations for the effective film are derived in section 3, with descriptions of both surface-like and guided modes. Their properties are investigated numerically in section 4 (symmetric film), and section 5 (asymmetric film). The conclusions are presented in section 6.

For numerical illustration we use parameters for the GaAs/AlAs system which are tabulated by Adachi (1985).

2. Bulk and surface modes

In a semi-infinite medium magnetoplasma polariton modes have been discussed in the non-retarded limit by a number of authors (e.g., Pakhomov and Stepanov (1967), Abdel-Shahid and Pakhomov (1970), and Chin and Quinn (1972)). In the retarded limit magnetoplasma modes have been investigated by, e.g., Brion *et al* (1973), Wallis *et al* (1974), Boardman *et al* (1977) and Aers *et al* (1978). In this section we consider the analogous situation for a semi-infinite effective medium.

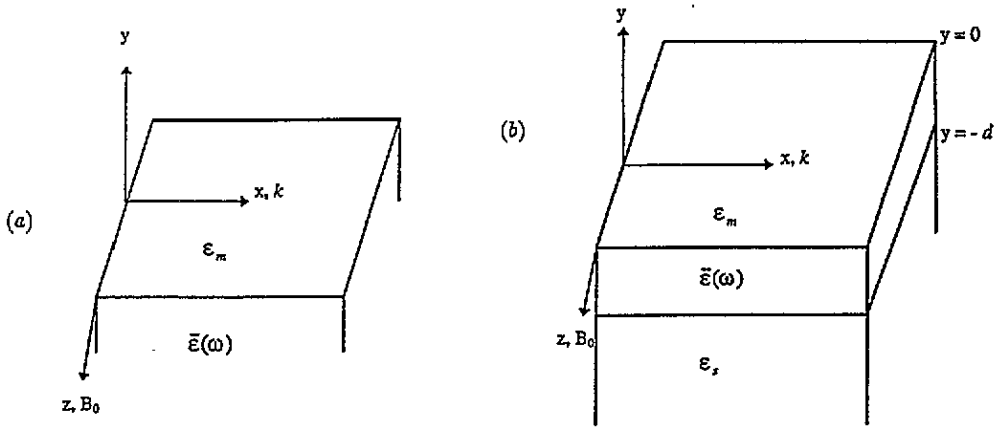

Figure 1. Schematic diagrams and choices of the axes for Voigt propagation: (*a*) surface; (*b*) effective film on substrate.

We employ the geometry shown in figure 1(*a*) where the effective medium fills the half space $y < 0$, with the surfaces of the films parallel to the x–z plane. We restrict our attention to the Voigt geometry, with the magnetic field B_0 along the z axis. The effective

dielectric tensor is given by (Agranovich 1991, Oliveros *et al* 1993, Elmzughi *et al* 1995)

$$\varepsilon(\omega) = \begin{pmatrix} \varepsilon_1 & -i\varepsilon_T & 0 \\ i\varepsilon_T & \varepsilon_2 & 0 \\ 0 & 0 & \varepsilon_3 \end{pmatrix} \tag{1}$$

where

$$\varepsilon_1 = f_a\varepsilon_1^a + f_b\varepsilon_2^b - f_a f_b(\varepsilon_2^a - \varepsilon_2^b)^2/(f_a\varepsilon_1^b + f_b\varepsilon_1^a) \tag{2a}$$

$$\varepsilon_2 = \varepsilon_1^a\varepsilon_1^b/(f_a\varepsilon_1^b + f_b\varepsilon_1^a) \tag{2b}$$

$$\varepsilon_3 = f_a\varepsilon_3^a + f_b\varepsilon_3^b \tag{2c}$$

and

$$\varepsilon_T = (f_a\varepsilon_2^a\varepsilon_1^b + f_b\varepsilon_2^b\varepsilon_1^a)/(f_a\varepsilon_1^b + f_b\varepsilon_1^a) \tag{2d}$$

where $f_a = (a/D)$ and $f_b = (b/D)$ are the volume fractions occupied by layers a and b, with D $(= a + b)$ the superlattice period. Here in the presence of a magnetic field B_0 along the z axis, the dielectric tensor $\varepsilon^\alpha(\omega)$ $(\alpha = a$ or $b)$ of each layer takes off-diagonal form (Boardman and Parker 1975), which can be derived from an extension of the classical Drude (Boardman 1982, Cottam and Tilley 1989) model and therefore has the form

$$\varepsilon^\alpha(\omega) = \begin{pmatrix} \varepsilon_1^\alpha & -i\varepsilon_2^\alpha & 0 \\ i\varepsilon_2^\alpha & \varepsilon_1^\alpha & 0 \\ 0 & 0 & \varepsilon_3^\alpha \end{pmatrix} \tag{3}$$

where

$$\varepsilon_1^\alpha = \varepsilon_\infty^\alpha(1 + \omega_p^{\alpha^2}/(\omega_c^{\alpha^2} - \omega^2)) \tag{4a}$$

$$\varepsilon_2^\alpha = \varepsilon_\infty^\alpha\omega_c^\alpha\omega_p^{\alpha^2}/\omega(\omega_c^{\alpha^2} - \omega^2) \tag{4b}$$

and

$$\varepsilon_3^\alpha = \varepsilon_\infty^\alpha(1 - \omega_p^{\alpha^2}/\omega^2). \tag{4c}$$

In the above, the cyclotron frequency is $\omega_c^\alpha = eB_0/m_\alpha^*$, and plasma frequency $\omega_p^{\alpha^2} = n_\alpha e^2/\varepsilon_0\varepsilon_\infty^\alpha m_\alpha^*$. Here n_α and m_α^* are the density and effective mass of the carriers. For simplicity we omit the optic phonon contributions; this is satisfactory as long as ω_p^α and ω_c^α are not close to the phonon resonances (Reststrahl region).

We consider p-polarized surface waves propagating perpendicular to an applied magnetic field. The previous derivation shows the bulk mode propagation transverse to B_0 with wavevector $k = (k, k_y, 0)$ (here we put $k_x = k$) follows from the wave equation and the mode frequencies satisfy (Oliveros *et al* 1993)

$$\beta^2 = -k_y^2 = ((\varepsilon_1/\varepsilon_2)k^2 - q_0^2\varepsilon_V) \tag{5}$$

where $\varepsilon_V = (\varepsilon_1\varepsilon_2 - \varepsilon_T^2)/\varepsilon_2$ is the Voigt permittivity, and $q_0^2 = \omega^2/c^2$. The frequency dependence of the real part of ε_V for various cases is illustrated by Oliveros *et al* (1993).

For surface modes, we consider next the interface between the magnetoplasma and the region with frequency-independent dielectric constant ε_m ($y > 0$ in figure 1(a)). The bulk polariton dispersion relation in this medium can also be derived from Maxwell's wave equation, viz.

$$\beta_m^2 = k^2 - q_0^2\varepsilon_m. \tag{6}$$

The surface polariton is localized at the interface, so that in both media β_m and β must be real. Clearly, for this condition to hold, (5) and (6) lead to the inequalities

$$k^2 > q_0^2 \varepsilon_m \tag{7}$$

$$k^2 > q_0^2 \varepsilon_V \varepsilon_2 / \varepsilon_1. \tag{8}$$

The conditions that the tangential components of $\boldsymbol{E}$ and the normal components of $\boldsymbol{D}$ should be continuous at the interface lead to the dispersion relation (Oliveros *et al* 1993)

$$\beta \varepsilon_m + \beta_m \varepsilon_V - \varepsilon_m (\varepsilon_T / \varepsilon_2) k = 0. \tag{9}$$

In (9) one can note that the third term is linear in k, so the dispersion graph $\omega(k)$ is non-reciprocal, $\omega(k) \neq \omega(-k)$ (see e.g., Camley 1987). As mentioned before, (7) and (8) define the regions of the ω–k plane in which the surface mode may exist. For illustration we consider only a vacuum interface ($\varepsilon_m = 1$) in all that follows. Equation (7) requires that k lies to the right of the vacuum light line.

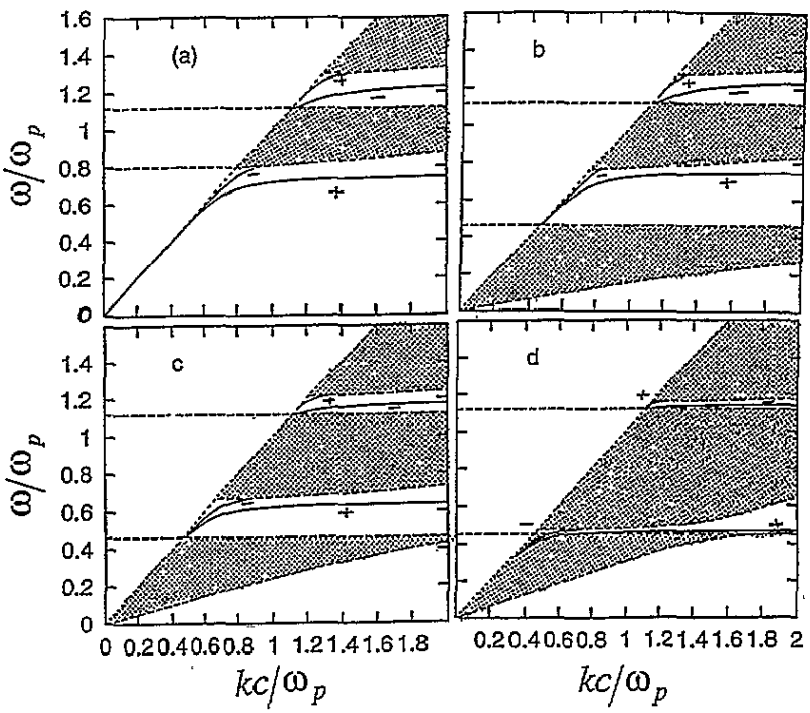

Figure 2. Dispersion relation curves ω versus k for bulk (shaded regions) and surface (solid lines) for a GaAs (doped)/AlAs (undoped) effective medium superlattice with (*a*) $f_a = 1$, (*b*) $f_a = 0.8$, (*c*) $f_a = 0.5$, and (*d*) $f_a = 0.2$.

Bulk and surface polariton dispersion curves calculated from (5) and (9) are shown in figure 2 for a GaAs (doped)/AlAs (undoped) superlattice. These are presented as graphs of ω/ω_p against kc/ω_p. Since the abscissa in figure 2 is k, (5) defines the continuum

$$k^2 < q_0^2 (\varepsilon_1 \varepsilon_2 - \varepsilon_T^2)/\varepsilon_1 \tag{10}$$

throughout which bulk modes can propagate with appropriate values of k_y. The number of bulk continuum regions (shaded areas in the graphs) is governed by the number of poles of $(\varepsilon_1 \varepsilon_2 - \varepsilon_T^2)/\varepsilon_1$; this means $k \to \infty$ on the positive side of the poles and there is no

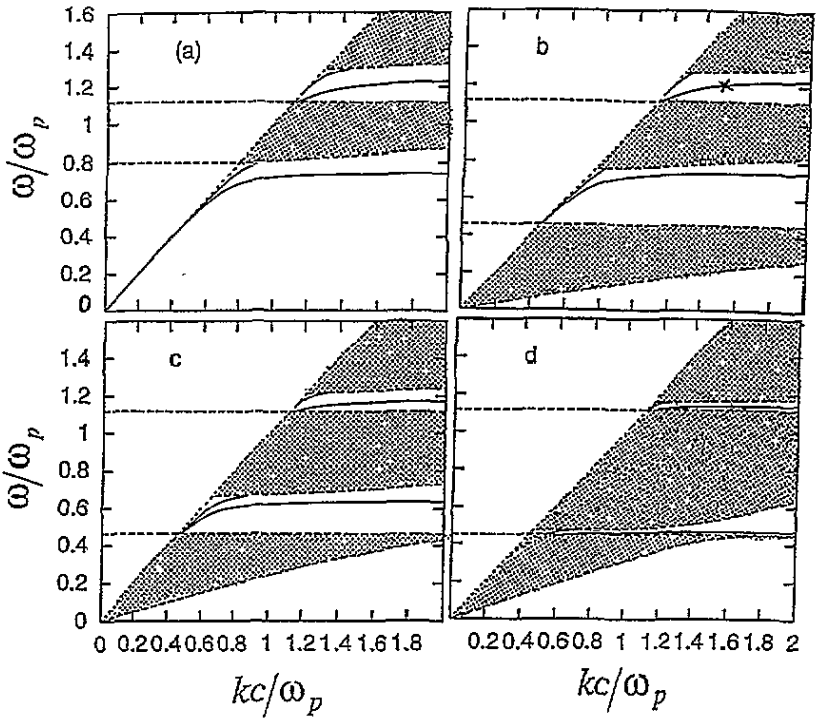

Figure 3. Dispersion relation curves ω versus k for bulk (shaded regions) and surface (solid lines) for a GaAs (doped)/AlAs (undoped) effective medium symmetric film with $d = 15$ μm, and $\omega/\omega_p = 0.5$: (*a*) $f_a = 1$, (*b*) $f_a = 0.8$, (*c*) $f_a = 0.5$, (*d*) $f_a = 0.2$.

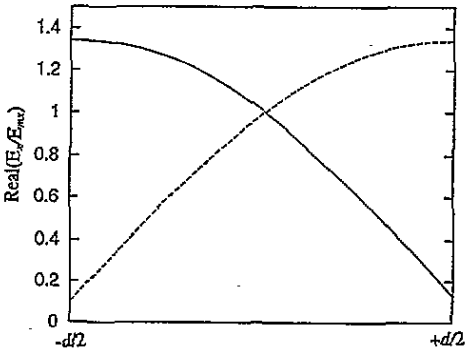

Figure 4. The field profiles for $+k$ (solid line) and $-k$ (dashed line) surface modes of the symmetric magnetoplasma effective film for $d = 15$ μm. These are drawn for the point $kc/\omega_p = 1.45$, $\omega/\omega_p = 1.18$ marked on the upper real surface mode curve in figure 3(*b*).

solution for k on the negative side of the poles. Figure 2(*a*) illustrates the case of $f_a = 1$ (bulk GaAs), where there are two bulk regions. When $f_a < 1$ the number of poles of $(\varepsilon_1\varepsilon_2 - \varepsilon_T^2)/\varepsilon_1$ increases, with a corresponding increase in the number of bulk regions; as depicted in figure 2(*b*)–(*d*). It is noted that the width of bulk regions in these curves increases as f_a decreases. The stop bands of the bulk modes are the surface windows. There are two windows in each part of figure 2 and, where the fraction f_a changes, these

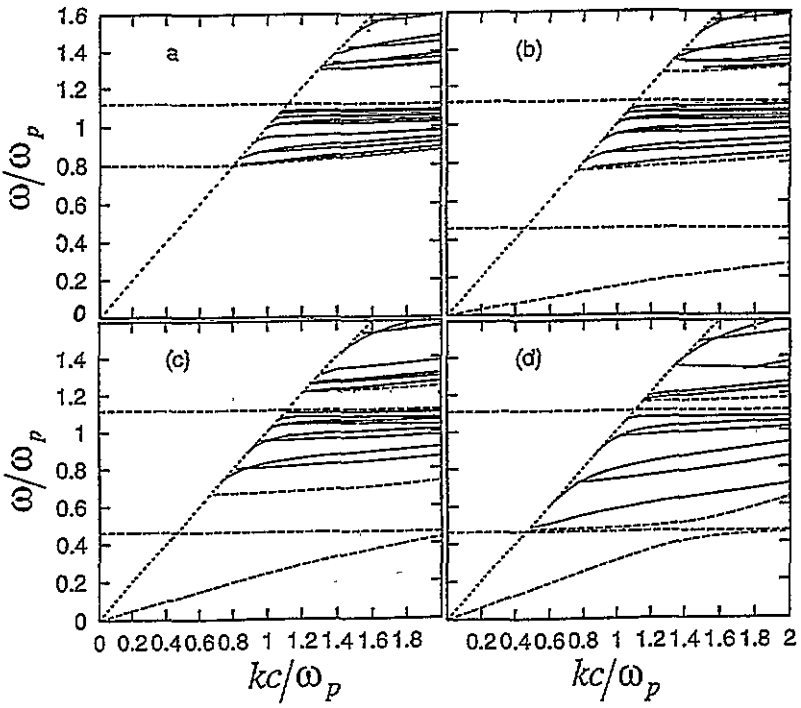

Figure 5. Guided wave dispersion curves ω versus k for an effective symmetric film with the same parameters as in figure 3, $d = 15$ μm: (*a*) $f_a = 1$, (*b*) $f_a = 0.8$, (*c*) $f_a = 0.5$, (*d*) $f_a = 0.2$.

windows decrease as well. The designations + or − correspond to $+k$ or $-k$ respectively. The non-reciprocity, that is the difference in frequency between the $+k$ and $-k$ modes, is clearly seen in figure 2. For each case two surface models are predicted. One is real with an electrostatic limit ($k \to \infty$), and the other is 'virtual', terminating at a finite value of k in the bulk continuum.

3. Effective film modes

We consider the geometry shown in figure 1(*b*). An effective magnetoplasma film is sandwiched between two dielectric media, the substrate characterized by dielectric constant ε_s and a capping layer having dielectric constant ε_m. For surface modes, Maxwell's equations are to be solved together with the electromagnetic boundary conditions at each interface. In this section we concentrate on the case of p-polarization. It is noteworthy that an s-polarized wave would lead to $\beta^2 = k^2 - q_0^2\varepsilon_3$. We write the field distributions in the three media in the form

$$\boldsymbol{H} = (0, 0, H_{mz}) \exp(\beta_m y) \qquad y > 0 \qquad (11)$$

$$\boldsymbol{H} = (0, 0, H_{1z}) \exp(\beta y) + (0, 0, H_{2z}) \exp(-\beta y) \qquad 0 > y > -d \qquad (12)$$

$$\boldsymbol{H} = (0, 0, H_{sz}) \exp(-\beta_s y) \qquad -d > y \qquad (13)$$

where $\exp(\mathrm{i}(kx - \omega t))$ is an implicit common factor in (11)–(13). Here the inverse penetration length β_s is given by a relation similar to (6). By employing the Maxwell equation $\nabla \times \boldsymbol{H} = -\partial \boldsymbol{D}/\partial t$ the electric fields in the three regions can be obtained. To

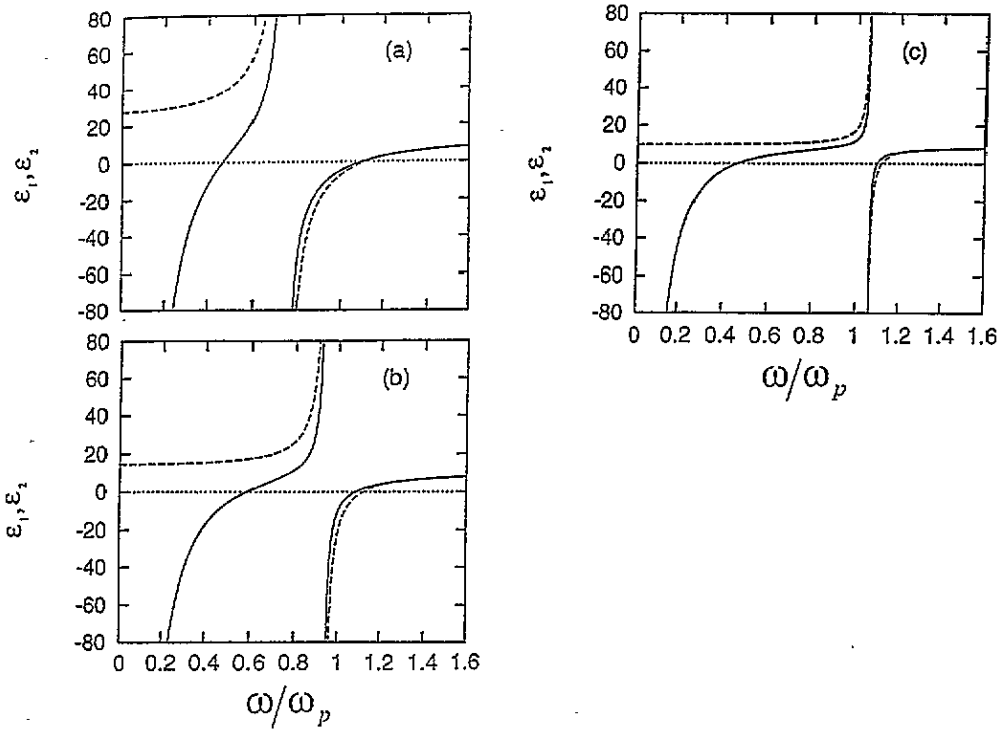

Figure 6. Permittivities ε_1 (equation (2*a*)) versus ω (solid lines) and ε_2 (equation (2*b*)) versus ω (dashed lines) with the same parameters as in figure 2: (*a*) $f_a = 0.8$, (*b*) $f_a = 0.5$, (*c*) $f_a = 0.2$.

obtain the surface polariton dispersion relation requires the matching of electromagnetic boundary conditions at each interface, namely continuity of the tangential components of electric and magnetic field E_x and H_z. Using Maxwell's curl equations, one can express E_x in terms of H_z. Then the boundary conditions at both interfaces yield four homogeneous equations for the four coefficients H_{mz}, H_{1z}, H_{2z}, and H_{sz}; the solvability condition yields after some algebra, the dispersion equation

$$[(\varepsilon_2\varepsilon_V\beta_m - \varepsilon_m g_+)/(\varepsilon_2\varepsilon_V\beta_m - \varepsilon_m g_-)]e^{-\beta d} = [(\varepsilon_2\varepsilon_V\beta_s - \varepsilon_s g_+)/(\varepsilon_2\varepsilon_V\beta_s - \varepsilon_s g_-)]e^{\beta d} \quad (14a)$$

which reduces to

$$(\beta_m\beta_s(\varepsilon_1\varepsilon_2 - \varepsilon_T^2) - k\varepsilon_T(\beta_s\varepsilon_m - \beta_m\varepsilon_s) + q^2\varepsilon_m\varepsilon_s)\tanh(\beta d) + \beta\varepsilon_2(\beta_s\varepsilon_m + \beta_m\varepsilon_s) = 0 \quad (14b)$$

where $g_\pm = i\varepsilon_T k \pm \varepsilon_2\beta$ and $q^2 = k^2 - q_0^2\varepsilon_2$. Equations (14) above constitute the main analytical results of the work. (14*a*) apart from the first term on the left-hand side, agrees with the expression for the non-effective film. When $f_a = 1$, (14*b*) reduces to the corresponding results of Kushwaha and Halevi (1987b) and Elmzughi and Tilley (1994). It is worth pointing out that the dispersion relation (14) reduces to (9) when $d \to \infty$, and for $d = 0$ yields the dispersion relation for surface polaritons propagating at the interface between two semi-infinite isotropic media (e.g. see Cottam and Tilley (1989)).

Depending upon position in the (k, ω) plane, β can be either pure imaginary (guided waves) or real (surface waves). In the electrostatic limit $k \gg q_0$, the decay constants reduce to $\beta_m = \beta_s = q = k$ and

$$\beta = (\varepsilon_1/\varepsilon_2)^{1/2}k. \quad (15)$$

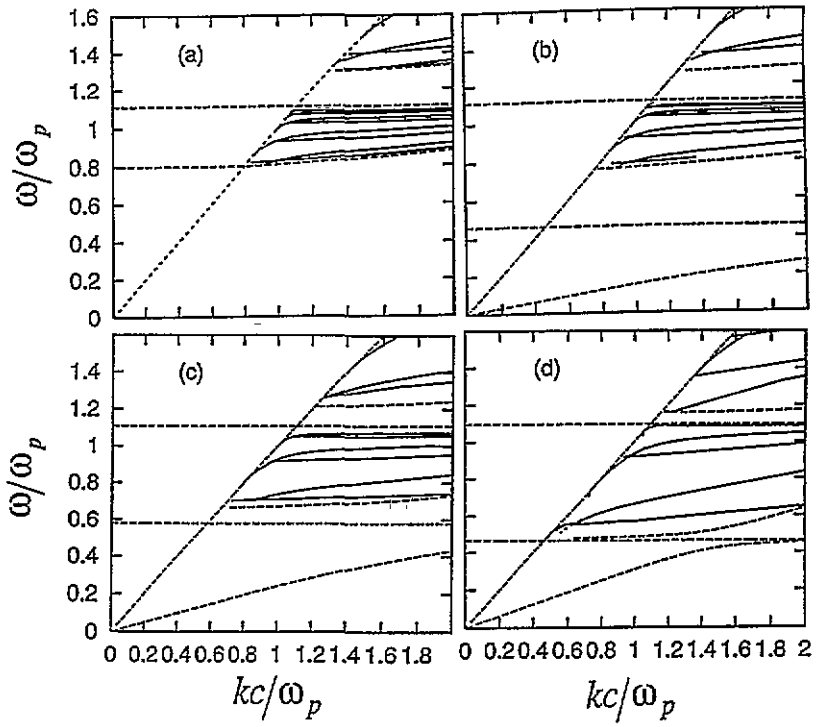

Figure 7. Guided wave dispersion curves ω versus k for an effective symmetric film with $d = 10$ μm. The other parameters are as given in figure 3. (*a*) $f_a = 1$, (*b*) $f_a = 0.8$, (*c*) $f_a = 0.5$, (*d*) $f_a = 0.2$.

Equation (14) then reduces to

$$(\varepsilon_1\varepsilon_2 - \varepsilon_T^2 + \varepsilon_m\varepsilon_s - \varepsilon_T(\varepsilon_m - \varepsilon_s))\tanh((\varepsilon_1/\varepsilon_2)^{1/2}kd) + (\varepsilon_1\varepsilon_2)^{1/2}(\varepsilon_m + \varepsilon_s) = 0. \tag{16}$$

It follows from (15) and (16) that ε_1 and ε_2 must both have the same sign in order to have modes in the electrostatic limit. We analyse (16) in the following two cases.

(i) $kd \gg 1$. The hyperbolic tangent in (16) tends to unity, hence (16) reduces to

$$(\varepsilon_1\varepsilon_2)^{1/2} + \varepsilon_T + \varepsilon_m = 0 \qquad \text{(for } +k\text{)} \tag{17}$$

$$(\varepsilon_1\varepsilon_2)^{1/2} - \varepsilon_T + \varepsilon_s = 0 \qquad \text{(for } -k\text{)}. \tag{18}$$

Equations (17) and (18) show that there are two solutions corresponding to $k \to \pm\infty$ for each of the interfaces in the electrostatic limit. (17) and (18) for $f_a = 1$ reduce to equations (19) in the paper by Kushwaha and Halevi (1987b). Also (17) and (18) in the same limit together with $d \to \infty$ reproduce exactly the results previously obtained by Pakhomov and Stepanov (1967).

(ii) $kd \ll 1$. Assuming that $(\varepsilon_1/\varepsilon_2)^{1/2}kd \ll 1$, then (16) yields an explicit solution for k

$$k = -(1/d)\varepsilon_2(\varepsilon_m + \varepsilon_s)/(\varepsilon_1\varepsilon_2 + \varepsilon_m\varepsilon_s - \varepsilon_T^2 - \varepsilon_T(\varepsilon_m - \varepsilon_s)). \tag{19}$$

This result holds for very thin films.

For the symmetric configuration, when ε_m and ε_s are both equal to, say, ε, (14*a*) divides into solutions in which the tangential components of the electric field (E_x) are either even

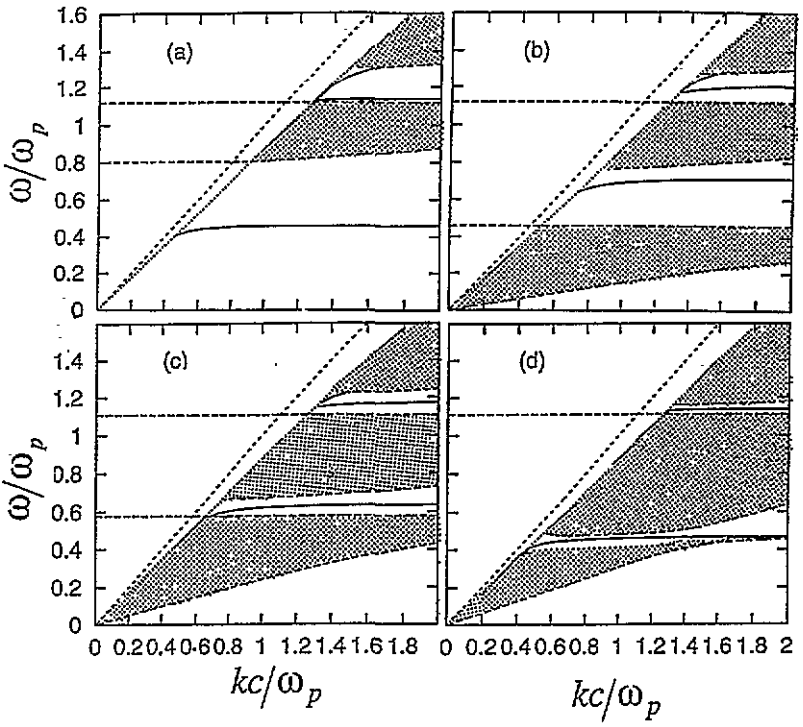

Figure 8. Dispersion relation curves ω versus k for bulk (shaded regions) and surface (solid lines) for a GaAs (doped)/AlAs (undoped) effective medium asymmetric film with $d = 15$ μm and $\omega/\omega_p = 0.5$. The bounding media have $\varepsilon_m = 1$ and $\varepsilon_s = 1.3$. The light lines $k = \omega/c$ and $k = \varepsilon_s^{1/2}\omega/c$ are shown. The guided windows are shaded; $+k$ propagation. (*a*) $f_a = 1$, (*b*) $f_a = 0.8$, (*c*) $f_a = 0.5$, (*d*) $f_a = 0.2$.

or odd about the centre of the film, with the two dispersion equations

$$(\beta_m\varepsilon_V)^2 + (\beta\varepsilon)^2 - ((\varepsilon\varepsilon_T/\varepsilon_2)k)^2 = -2\varepsilon\varepsilon_V\beta_m\beta\tanh(\beta d) \qquad \text{(odd)} \quad (20)$$

$$(\beta_m\varepsilon_V)^2 + (\beta\varepsilon)^2 - ((\varepsilon\varepsilon_T/\varepsilon_2)k)^2 = -2\varepsilon\varepsilon_V\beta_m\beta\coth(\beta d) \qquad \text{(even)}. \quad (21)$$

As $d \to \infty$, the hyperbolic functions in (20) and (21) tend to unity, and both equations are asymptotically the same as the dispersion relation for the single interface mode (9) with $\varepsilon = 1$.

4. Symmetric films

We start by discussing the bulk and surface-type modes of symmetric effective films where (20) and (21) hold (β real). Surface mode windows are the stop bands of the bulk modes (5). Since k appears only as k^2 in (20) and (21), the surface modes exhibit reciprocal propagation. The reason, as discussed by Elmzughi and Tilley (1994), can be seen by considering the vectors $\boldsymbol{n}_m \times \boldsymbol{B}_0$ and $\boldsymbol{n}_s \times \boldsymbol{B}_0$ where $\boldsymbol{n}_m$ is the normal to the upper surface of the film and $\boldsymbol{n}_s$ is the normal to the lower surface of the film, these being in opposite directions. Therefore the surface-type modes that propagate in the $\pm x$ direction have $\pm k$ on the vacuum/film interface, but $\mp k$ on the substrate/film interface. The detailed form of the solution depends on the value of the film thickness d. When $d \to \infty$, the hyperbolic

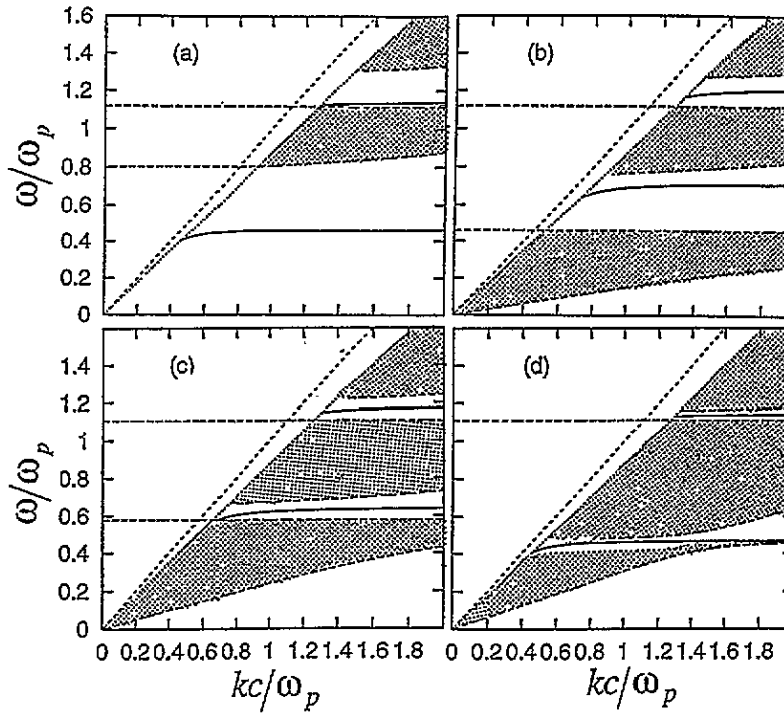

Figure 9. Dispersion relation curves ω versus k for bulk (shaded regions) and surface (solid lines) for a GaAs (doped)/AlAs (undoped) effective medium asymmetric film with $d = 15$ μm and $\omega/\omega_p = 0.5$. The bounding media have $\varepsilon_m = 1$ and $\varepsilon_x = 1.3$. The light lines $k = \omega/c$ and $k = \varepsilon_x^{1/2}\omega/c$ are shown. The guided windows are shaded; $-k$ propagation. (*a*) $f_a = 1$, (*b*) $f_a = 0.8$, (*c*) $f_a = 0.5$, (*d*) $f_a = 0.2$.

functions in (20) and (21) tend to unity and both equations read

$$(\beta_m \varepsilon_V + \beta\varepsilon)^2 - ((\varepsilon\varepsilon_T/\varepsilon_2)k)^2 = 0 \tag{22}$$

which is the same as (9). When $f_a = 1$, (22) reduces to equation (21) of Elmzughi and Tilley (1994), and if $\varepsilon = 1$, (22) is just the product of the $+k$ and $-k$ forms of (9). Therefore in thin films (20) and (21) describe the plus and minus surface-type modes on the top and bottom film surfaces. The dispersion curves of the surface modes for a 15 μm symmetric effective film made, e.g. from 1500 layers of GaAs/AlAs, with superlattice period 100 Å, are shown in figure 3. These curves are seen to be similar to those for a single interface (figure 2). Here we have not marked the surface modes as + and − modes, because both modes are found with either $\pm k$. All upper modes in each window in figure 3 are virtual, while the lower ones are real surface modes as in figure 2. All the surface modes start at their low-frequency end on the vacuum light line $\omega = ck$.

Although the dispersion curves are reciprocal, the localization of the modes is not. This can be seen from the field profiles for the surface-type modes. It is convenient to represent the field profile by evaluating $\mathrm{Re}(E_x/E_{mx})$, in other words, the real part of the ratio of the parallel electric field in the effective medium (E_x) to that in the capping layer (E_{mx}). These components of fields can be determined from (11) and (12). When ω and k are known (11) and (12) can be solved for the ratios E_{1x}/E_{mx} and E_{2x}/E_{mx}, therefore the field profile can be determined. An example is illustrated in figure 4 for the $+k$ and $-k$ modes at the point

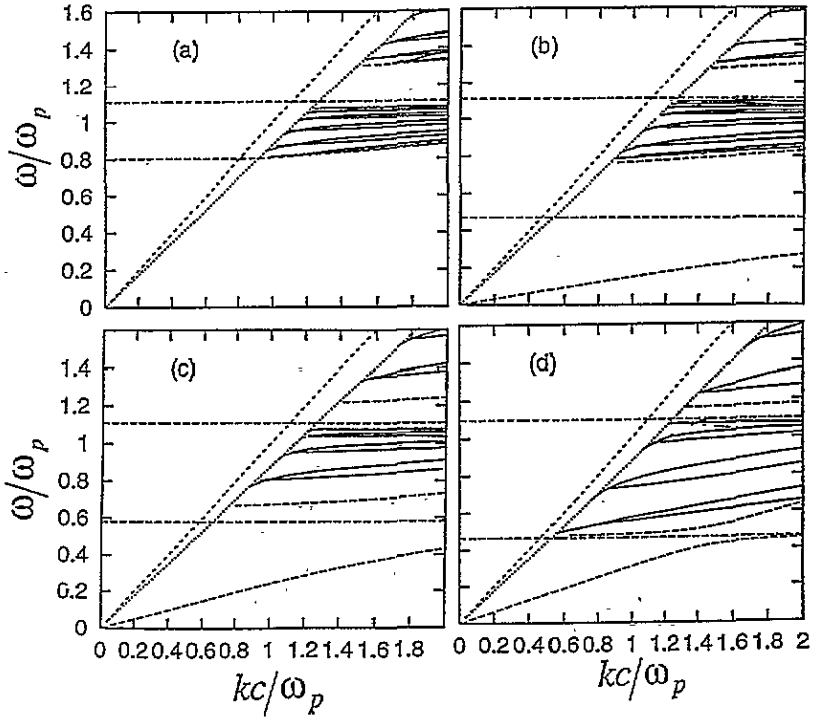

Figure 10. Guided wave dispersion curves ω versus k for an effective asymmetric film with $d = 15$ μm. The other parameters are the same as in figure 7. (*a*) $f_a = 1$, (*b*) $f_a = 0.8$, (*c*) $f_a = 0.5$, (*d*) $f_a = 0.2$.

marked $\times$ in figure 3(*b*). In figure 4, in agreement with the above arguments, the $+k$ mode is localized at $y = -d/2$ whilst the $-k$ mode is localized at $y = +d/2$.

The shaded areas in figure 3, which are the same as in figure 2, are bulk continua. These are the guided wave windows. The guided wave modes of the symmetric effective films are the solutions of (20) and (21) with β pure imaginary. They exist in the windows defined by (7) together with

$$k < q_0^2 \varepsilon_V \varepsilon_2 / \varepsilon_1. \tag{23}$$

For the same reason as for the surface modes, the guided mode dispersion relations are reciprocal but the field profiles are not. The numerical results for the guided modes are illustrated in figure 5 for the same symmetric films as in figure 3. For the case of $f_a = 1$ (bulk GaAs), figure 5(*a*), the guided modes appear in all guided wave windows, but when $f_a < 1$ the guided modes appear only in the two upper guided windows, and do not exist in the lower windows. The reason can be seen from figure 6, which shows the permittivities ε_1 and ε_2 against frequency for the values of f_a in figure 5(*b*)–(*d*). In these curves ε_1 is negative in the frequency ranges of the lower guided windows. In these ranges β does not satisfy the guided wave condition. The spacing of the guided type modes depends on the values of the volume fractions f_a and f_b; when $f_a < 1$ (doped layer) the dispersion curves are more widely spaced, as can be seen in figure 5. Also the spacing of the guided-type modes depends on the value of the film thickness d, and the dispersion curves are more widely spaced for small d. This can be seen in figure 7 for $d = 10$ μm in comparison with figure 5 for $d = 15$ μm, which shows the characteristic wider spacing of the curves for the thinner film.

5. Asymmetric films

The asymmetric film is a film on a substrate, and this case occurs more frequently in practice. Some differences accrue in the dispersion curves compared with the symmetric case. We return to the general dispersion equation (14), and consider $\varepsilon_m \neq \varepsilon_s$; the dispersion is consequently non-reciprocal. As seen in figure 4 for the symmetric effective films, although the propagation is reciprocal, the field profiles are different for $+k$ and $-k$. A second property is that in the asymmetric effective film the modes no longer have a definite parity about the midpoint of the film.

The bulk and surface-type modes for the asymmetric effective film are illustrated in figure 8 for the case of $+k$ propagation, where real surface modes appear in all surface windows. Virtual surface modes also appear in the upper surface windows as shown in figure 8(a)–(c) for the case $f_a > 0.5$. Figure 9 shows the case of $-k$ propagation for the same films as in figure 8. The non-reciprocity can be seen in the comparison between these two figures. It is also seen that the introduction of a substrate ($\varepsilon_m \neq \varepsilon_s$) removes the virtual modes for $+k$ propagation. One can note in asymmetric films the surface modes start at their low-frequency end on the light line of substrate $\omega = \varepsilon_s^{1/2} ck$.

The guided wave modes for the same effective films are illustrated in figure 10 for the case of $+k$. Examination of the data files for $+k$ and $-k$ shows that the propagation is non-reciprocal but the differences are too small to show clearly on the graphs.

6. Conclusion

We have applied the theory of the effective medium to discuss retarded electromagnetic modes of an effective superlattice film, with graphical results shown for the GaAs (doped)/AlAs (undoped) system. In order to focus on features that are specifically related to the magnetic field we have omitted Reststrahl dispersion from the underlying dielectric constant.

We have given a full account for the surface and guided wave polariton modes of a magnetoplasma *effective* film for the first time. The main new results are the surface polariton dispersion equations (14) and curves for the Voigt configuration, sections 3–5, compared with the magnetoplasma film (Elmzughi and Tilley 1994). In the effective films one of the guided-type modes does not appear in some of the guided windows. This can be understood from the response of the dielectric tensor to the electromagnetic waves.

The most obvious technique to investigate the magnetoplasma modes discussed here is attenuated total reflection (ATR). Expressions for ATR reflectivity could be derived and computed without undue difficulty from the effective dielectric tensor under the considered geometry. Substantial information about the dielectric tensor itself can be obtained by means of simpler techniques, for example oblique incidence reflectivity (Dumelow *et al* 1993). Here again, the relevant expressions could be derived in a straightforward way.

Acknowledgments

I am grateful for helpful discussion with Professor Rodney Loudon, Professor D R Tilley and Dr N C Constantinou. I acknowledge financial support from Al-Fatah University.

References

Abdel-Shahid N Z and Pakhomov V I 1970 *Plasma Phys.* **12** 55
Adachi S 1985 *J. Appl. Phys.* **58** R1
Aers G C, Boardman A D and Clark P 1978 *Phys. Status Solidi* b **85** 171
Agranovich V M 1991 *Solid State Commun.* **78** 747
Agranovich V M and Kravstov V E 1985 *Solid State Commun.* **55** 85
Boardman A D 1982 *Electromagnetic Surface Modes* ed A D Boardman (Chichester: Wiley)
Boardman A D, Isaac E D, Lissberger P H and Aers G C 1977 *Physica* B **89** 119
Boardman A D and Parker M R 1975 *Phys. Status Solidi* b **71** 329
Brion J J, Wallis R F, Hartstein A and Burstein E 1973 *Surf. Sci.* **34** 73
Camley R E 1987 *Surf. Sci. Rep.* **7** 103
Chin K W and Quinn J J 1972a *Phys. Rev.* B **5** 4707
——1972b *Nuovo Cimento* B **10** 1
Cottam M G and Tilley D R 1989 *Introduction to Surface and Superlattice Excitations* (Cambridge: Cambridge University Press)
Dumelow T, Parker T J, Smith S R P and Tilley D R 1993 *Surf. Sci. Rep.* **17** 151
Dumelow T and Tilley D R 1993 *J. Opt. Soc. Am.* A **10** 633
Elmzughi F G, Constantinou N C and Tilley D R 1995 *J. Phys.: Condens. Matter* **7** 315
Elmzughi F G and Tilley D R 1994 *J. Phys.: Condens. Matter* **6** 4233
Kushwaha M S and Halevi P 1987a *Phys. Rev.* B **35** 3879
——1987b *Phys. Rev.* B **36** 5960
——1987c *Solid State Commun.* **64** 1405
——1988 *Phys. Rev.* B **38** 12 428
Oliveros M C, Almeida N S and Tilley D R 1993 *Semicond. Sci. Technol.* **8** 441
Pakhomov V I and Stepanov K N 1967 *Zh. Tekh. Fiz.* **37** 1393
Raj N and Tilley D R 1985 *Solid State Commun.* **55** 373
——1989 *The Dielectric Function of Condensed Systems* ed L V Keldysh, D A Kirzhnitz and A A Maradudin (Amsterdam: Elsevier) ch 7
Wallis R F, Brion J J, Burstein E and Hartstein A 1974 *Phys. Rev.* B **9** 3424